Evidence for the Formation of Different Energetically Similar Atomic Structures in Ag(111)-($\sqrt{7} \times \sqrt{7}$)-*R*19.1°-CH_3S

D. Torres,[1] P. Carro,[2] R. C. Salvarezza,[3] and F. Illas[1]

[1]*Departament de Química Física and CeRQT, Universitat de Barcelona and Parc Científic de Barcelona, E-08028 Barcelona, Spain*
[2]*Departamento de Química Física, Universidad de La Laguna, Tenerife, Spain*
[3]*Instituto de Investigaciones Fisicoquímicas Teóricas y Aplicadas-UNLP-CONICET, Sucursal 4 Casilla de Correo 16 (1900) La Plata, Argentina*

(Received 3 July 2006; published 30 November 2006)

The atomic structure and thermodynamic stability of Ag(111)($\sqrt{7} \times \sqrt{7}$)-*R*19.1°-CH_3S has been studied by means of density functional calculations and atomistic first principles thermodynamics. The unreconstructed model and two recently proposed reconstructions have been considered. It is found that, in spite of significant differences in the atomic structure, the different surface models have a very similar surface free energy. It is claimed that the different ordered phases can coexist and that the appearance of one or another depends on the external preparation conditions.

DOI: 10.1103/PhysRevLett.97.226103 PACS numbers: 81.16.Dn, 68.43.Hn, 68.55.−a, 71.15.−m

Self-assembled monolayers (SAMs) of *n*-alkanethiols [$CH_3(CH_2)_{n-1}SH$; C_n hereafter] on metals attract scientific interest and become technologically relevant targets because they provide an easy and controlled way to create surfaces with specific chemical functionalities [1]. Alkanethiols SAMs form through the S heads forming strong alkanethiolate-metal bonds [2]. Interaction between the neighbor hydrocarbon chains plays an important role in the self-assembly process and on the final structure of the SAM [3]. Thus, alkanethiolate monolayers on metal, mainly Ag and Au, surfaces constitute appropriate model systems for the study of fundamental aspects of the self-assembling process. SAMs usually form well ordered patterns [1], but the precise atomic structure for the simplest possible alkanethiol (CH_3S) is a matter of debate [4]. Control at the atomic level seems an unavoidable requirement for possible technological applications.

Alkanethiol adsorption on Au(111) leads to a stable SAM described by a ($\sqrt{3} \times \sqrt{3}$)-*R*30° unit cell [5], but a completely different packing of the alkyl chain is found for Ag(111). Moreover, information concerning the molecular structure and periodicity of the resulting monolayers is scarce and even contradictory [4]. There is clear evidence that CH_3S on Ag(111) forms a ($\sqrt{7} \times \sqrt{7}$)-*R*19.1° pattern [6,7]. However, this structure is compatible with more than one atomic arrangement. The simplest one (hereafter referred to as U in Fig. 1) corresponds to binding one-third of the S atoms on top sites and the rest on alternate hpc and fcc hollow sites of the unreconstructed Ag(111) lattice. Yu *et al.* [4] have very recently questioned this atomic model for the Ag(111)($\sqrt{7} \times \sqrt{7}$)-*R*19.1°-CH_3S structure and, based on a careful analysis of the normal incidence x-ray standing waves (NIXSWs), provided compelling evidence that the underlying metallic surface is strongly reconstructed. Yu *et al.* [4] found out that to fit the NIXSW data requires a near-hexagonal Ag surface layer with reduced atomic density so that it is 3/7 of the underlying substrate layers and that adsorbed CH_3S occupy three different sites on the surface unit cell (model A in Fig. 1). To justify the corrugated periodicity observed by STM [8], Yu *et al.* propose a second structure (model B in Fig. 1) differing from A only in a small displacement of the low coordinated Ag atoms. Clearly, a more detailed microscopic description of the different atomic structures proposed for the Ag(111) ($\sqrt{7} \times \sqrt{7}$)-*R*19.1°-CH_3S pattern is needed addressing the different energetic stability of the different models and the molecular structure of the adsorbed thiolate.

The present Letter aims to supply unbiased answers to these questions by means of accurate density functional (DF) calculations carried out on appropriate periodic models. From the DF energies, an analysis of the thermodynamical stability of the three ordered overlayers is presented by following the first principle atomistic thermodynamics formalism of Reuter and Scheffler [9]. We provide compelling evidence that, although the unreconstructed and reconstructed surface models present large differences in geometry and adsorption energy, they show

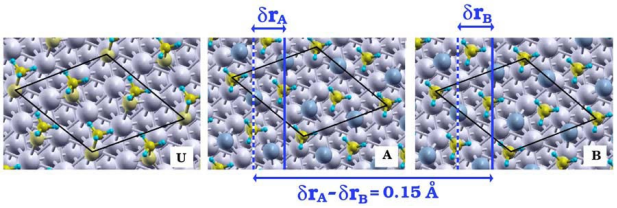

FIG. 1 (color online). Schematic plan view of the different surface models considered for the U, A, and B atomic models of the ($\sqrt{7} \times \sqrt{7}$)*R*19.1°-CH_3S phase. The vertical line indicates the displacement of the surface silver atoms of the reconstructed B model relative to A. The Ag atoms of the topmost atomic layer of the A and B models are presented in a darker color to facilitate the view. The main structural difference between the A and B initial models is highlighted; the final optimized geometries are almost identical.

a similar thermodynamic stability. We argue that depending on the external conditions and preparation one can favor one or the other without a precise control.

For the U model, taken until very recently [4] as the correct structure, a slab model with five metallic layers and three CH_3S molecules per unit cell has been used. One of the three CH_3S moieties is placed in an on-top site, whereas the two other adsorbates are placed one in the fcc and one in the hcp site. For the A and B structures, we start from the proposal of Yu *et al.* [4], and the topmost atomic layer has a reduced density of three silver atoms per surface unit cell, the remaining layers having the bulk density as in the U model. The surface Ag atoms were placed at equivalent low symmetry sites of the nonreconstructed adjacent layer. In all cases, CH_3S molecules sit above top, fcc, and hcp hollow sites; each CH_3S molecule is coordinated to three Ag atoms (Fig. 1). Thus, the resulting unit cells for the U, A, and B models contain 35, 31, and 31 Ag atoms plus three CH_3S, respectively. Notice that the only previous DF calculations for the $CH_3S/Ag(111)$ system have been carried out for an unrealistic $(\sqrt{3}\times\sqrt{3})$-$R30°$-CH_3S lattice never observed in the experiments [10].

The total energy and optimized geometry for the three U, A, and B structures have been obtained using the Perdew-Wang [11] implementation of the generalized gradient approach for the *xc* potential, using a lattice parameter optimized for the bulk metal (4.159 Å against experimental value of 4.085 Å [12]) and keeping it fixed in all calculations. The one-electron wave functions were expanded on a plane wave basis set with a cutoff of 420 eV. The projector augmented wave method [13] has been employed to describe the effect of the inner cores of the atoms on the valence electrons. The tolerance used to define self-consistency is 10^{-4} eV for the single-point total energy and 10^{-3} eV for the geometry optimization. The variational energy minimization for a given nuclear configuration is carried out using a Davidson-Bloch iteration scheme. The influence of the Brillouin zone sampling, according to the Monkhorst-Pack [14] scheme, and of vacuum width between the repeated slabs was investigated for the U model. Full geometry optimization of the three outermost atomic metal layers and of the atomic coordinates of all atoms in the three CH_3S molecules without further constraints was carried out with grids varying from $3\times3\times1$ to $9\times9\times1$ indicate that the bonding energy [see Eq. (1) below] is converged up to 0.03 eV. This small change in the adsorption energies with respect to the *k*-point grid results in modifications of the surface free energy plots of $\sim$1 meV/Å^2. A similar variation is found when the vacuum width is varied between the equivalent of 5 and 12 atomic layers. Therefore, calculations for the A and B models were carried out using the $3\times3\times1$ mesh and a 5 atomic layer vacuum width. All calculations have been carried out using the VASP package [15].

For coherence with the thermodynamic analysis below, we define the average binding energy (E_b) per thiolate adsorbed molecule in the Ag(111) $(\sqrt{7}\times\sqrt{7})$-$R19.1°$-CH_3S models with respect to the dimethyl disulfide—$(CH_3S)_2$—molecule as

$$E_b = \frac{1}{N_{CH_3S}}\left[E^{CH_3S/Ag} - E^{Ag} - N_{CH_3S}\frac{E^{(CH_3S)_2}}{2}\right], \quad (1)$$

where N_{CH_3S} is the number of thiolate molecules in the surface unit cell (3 in all cases), and $E^{CH_3S/Ag}$, E^{Ag}, and $E^{(CH_3S)_2}$ are the total energies of the adsorbate-substrate system, the clean surface, and the dimethyl disulfide molecule, respectively. Negative numbers indicate exothermic adsorption with respect to the clean surface and $(CH_3S)_2$. In principle, the larger E_b, the larger the stability of the resulting overlayer is. However, this reasoning cannot be used to differentiate the relative stability of the three Ag(111) $(\sqrt{7}\times\sqrt{7})$-$R19.1°$-CH_3S structures since it does not include the energy cost for the surface reconstruction in the A and B models. To compare the stability of the three different models, we make use of the surface free energy. To represent realistic thermodynamic conditions, we consider the surface in contact with a $(CH_3S)_2$ atmosphere at a given pressure and temperature. The $(CH_3S)_2$ molecules in the gas phase act as a reservoir interchanging molecules with the surface. Defining the chemical potential of the adsorbate with respect to the $(CH_3S)_2$ molecule as $\Delta\mu = \mu - \frac{1}{2}g_{(CH_3S)_2}$ permits one to include P and T implicitly. The Gibbs free energy of the dimethyl disulfide in the gas phase [$g_{(CH_3S)_2}$] has been computed as usual [9] from the total energy and the vibrational contributions to the zero point energy and entropy. The definition of $\Delta\mu$ permits one to write an expression for the surface free energy of the total system which takes into account the amount of $(CH_3S)_2$ in the gas phase:

$$\gamma(\Delta\mu) = \frac{1}{A}[E^{CH_3S/Ag} - N_{Ag}E^{Ag}_{Bulk} - N_{CH_3S}\Delta\mu] - \gamma_{clean} + \gamma^{vib}, \quad (2)$$

where A is the surface area; N_{Ag} and E^{Ag}_{Bulk} are the number of silver atoms in the slab unit cell (35 for U and 31 for A and B) and the total energy of bulk Ag, respectively; γ_{clean} is the surface free energy of the unreconstructed Ag(111) surface which has to be substracted because the slab model exhibits two surfaces, one unreconstructed and without adsorbate and another one with adsorbate and reconstructed or not depending on the case; and γ^{vib} accounts for the vibrational contributions due to both energy and entropy [9]. Finally, notice that the term corresponding to volume change is neglected since its contribution to g is very small ($\sim$1 meV/Å^2). The analysis of $\gamma(\Delta\mu)$ provides a clean and unbiased way to compare the relative stability of the three different Ag(111) $(\sqrt{7}\times\sqrt{7})$-$R19.1°$-CH_3S structures. Although this formalism can also be used to account for coverage effects, notice that the three structures considered in the present work are identical indepen-

dently of $\Delta\mu$. Consequently, plots of $\gamma(\Delta\mu)$ versus $\Delta\mu$ for the U, A, and B structures will be parallel.

The geometric parameters characterizing the U, A, and B structures are summarized in Table I. The final geometries for the metallic slabs are very close to the starting ones with a small first to second layer (d_{12}) relaxation only. For the U model, d_{12} is almost negligible and for A and B does not even reach 1%. Despite this small surface relaxation, there are rather large differences concerning the bonding mode and geometry of the adsorbate to the surface. For the U model, the perpendicular distance from the surface to the S head of CH_3S (z_e) ranges from ~1.9 Å for the threefold hollow sites to ~2.4 Å for the atop one. However, z_e is dramatically different in the A and B reconstructed phases where it ranges from 0.6 to ~0.7 Å. This overwhelmingly shorter distance between the surface and the adsorbate reflects the decrease of compactness of the metallic topmost atomic layer in the reconstructed models. Another striking difference between the U and A or B phase concerns the tilt of the C-S bond with respect to the surface. For the U structure, the $\angle$(surface, S, C) angle formed between the perpendicular to the surface and the C-S axis lies between 147° for the molecules at the threefold hollow sites and 123° for that on the on-top site. This orientation suggests a tetrahedral S atom with an sp^3 hybridization thus forming two bonds and having two lone pairs pointing away from the surface to reduce Pauli repulsion. The orientation of the CH_3S moiety for the A and B models is completely different, the S-C axis being almost perpendicular to the surface with a concomitant $\angle$(surface, S, C) angle of nearly 180°. This different orientation suggests an sp hybridization for the S atom with the two sp hybrid orbitals pointing towards the surface and the C atom, respectively, and with the two lone pairs lying parallel to the surface conferring perhaps a multiple bond character to the interaction, which is consistent with the much shorter z_e value in the A and B structures. Apart from the differences in z_e and $\angle$(surface, S, C), the internal molecular geometry of the CH_3S species is almost indistinguishable from that for the species in the gas phase, the only noticeable difference being a slight increase in the S-C distance of ~0.1 Å as expected from bond order conservation arguments. The computed geometry for the CH_3S species is very similar to that reported in previous work [10] using a similar DF approach.

Next, we discuss the resulting average E_b values for the U, A, and B models. For the U model, the average binding energy is quite small (−0.28 eV), but the corresponding value for the A and B models is nearly 3 times this value (−0.75 eV). Notice that these values are referred to $(CH_3S)_2$ and that to obtain values referred to CH_3S it is enough to add −1.5 eV, the resulting values being in agreement with experiment [16]. The increase in E_b for both reconstructed phases is due to the lack of coordination of the metal atoms in the lower density silver atomic topmost layer. However, a larger E_b does not necessarily mean a more stable structure, because the surfaces are different and the energy cost to reconstruct the clean surface needs to be taken into account. This is included in the surface free energy formalism outlined above. Figure 2 reports the surface free energy [$\gamma(\Delta\mu)$] for the U, A, and B structures as a function of the chemical potential difference with respect to half the Gibbs energy of $(CH_3S)_2$. The corresponding plots are linear, as expected from Eq. (2), and they are parallel, as expected for ordered overlayers with identical coverage. Before discussing the results summarized in Fig. 2 in some more detail, it is important to mention that the vibrational contribution to surface free energy makes an important part of the final $\gamma(\Delta\mu)$ value. However, γ^{vib} (at 300 K) is almost the same for the three structures, and since this, and also γ^{clean}, appear as independent terms in Eq. (2), these terms do not play any differential role in the relative stability of the U, A, and B phases. Also, since the slope of the three lines for $\gamma(\Delta\mu)$

TABLE I. DF predicted parameters for the U, A, and B ($\sqrt{7}\times\sqrt{7}$)-$R19.1°$-CH_3S structures. E_b—average adsorption energy of CH_3S as in Eq. (1); d_{12}—first interlayer distance; z_e(S)—average perpendicular distance from the S atom of adsorbed CH_3S to the surface for each site; r(S-Ag), r(S-C)—interatomic average S-Ag and S-C distances; $\angle$(S-C-H), $\angle$(surface, S, C)—S-C-H bonding angle and angle formed between the perpendicular to the surface plane and the S-C bond axis.

Parameter	U	A	B
E_b (eV)	−0.28	−0.75	−0.74
d_{12} (%)	−0.03	0.62	1.04
z_e(S) (Å)	1.883	0.651	0.736
r(S-Ag) (Å)	2.537	2.662	2.642
r(S-C) (Å)	1.834	1.836	1.844
$\angle$(S-C-H) (deg)	108	110	110
$\angle$(surface, S, C) (deg)	147	178	175

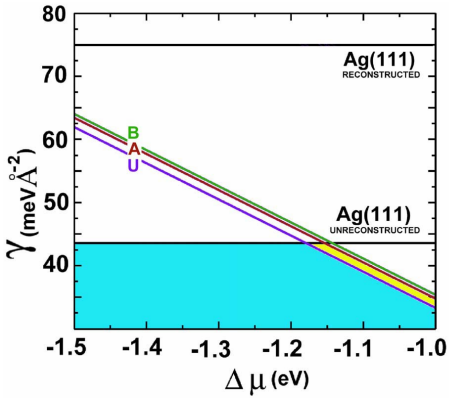

FIG. 2 (color online). Surface Gibbs free energy plot as a function of the CH_3S chemical potential with respect to $(CH_3S)_2$ for different U, A, and B surface models of the ($\sqrt{7}\times\sqrt{7}$)$R19.1°$-CH_3S phase. The horizontal lines indicate the surface free energy of the reconstructed and unreconstructed clean silver surfaces.

is the same, the relative stability is independent of the chemical potential of the adsorbate, which can be set arbitrarily to zero. Therefore, the relative stability of the different ordered phases is governed solely by the total energy of the total system relative to the Ag bulk. Although the relative stability does not depend on the chemical potential of the adsorbate, it is worth pointing out that in the limit of low $(CH_3S)_2$ partial pressures—left-hand side in Fig. 2—the clean Ag(111) surface exhibits the lowest surface free energy and is, hence, more thermodynamically stable than the ordered U, A, and B structures. When the CH_3S chemical potential with respect to $(CH_3S)_2$ increases (up to ~ -1.17 eV), the thermodynamic equilibrium is reached for the $(\sqrt{7}\times\sqrt{7})R19.1°$ structures, which is in agreement with the spontaneous formation of the SAMs. Now we come to the most important result of the present work, namely, the relative stability of the unreconstructed and of the A and B models proposed by Yu *et al.* [4] for the $(\sqrt{7}\times\sqrt{7})R19.1°$ periodic overlayer. In spite of the different number of atoms in the unit cell and of the very different surface topology of the topmost atomic layer, the surface free energy of the three models lie in a very narrow range; the absolute difference being less than 2 meV $Å^{-2}$. The reason for such unexpected behavior is the energy compensation between the cost to form the reconstructed Ag surface (cf. Figure 2) and the energy gain due to a more favorable adsorption of the CH_3S species (Table I). Therefore, one must conclude that depending on the preparation conditions one may find one or another structure with almost the same probability. The situation here is reminiscent of that recently reported for O on Ag(111) where structurally different phases exhibit a similar thermodynamic stability [17] but not been reported for SAMs or similar systems. We claim this is also the reason why Yu *et al.* [4] found a different atomic structure and also that the unreconstructed $(\sqrt{7}\times\sqrt{7})R19.1°$ model cannot be discarded. Note that the atomic corrugation described by Yu *et al.* [4] (model B) was not reported in other STM studies of alkanethiolate on Ag(111) where $(\sqrt{7}\times\sqrt{7})R19.1°$ was observed [2]. The possibility that reconstructed and unreconstructed domains coexist on the sample or during the self-assembly process also cannot be excluded. It could explain why the tilt angle experimentally observed ranges from 165° to 173° [18]. In fact, we have calculated 140°–150° for U, 178°–180° for A, and 175°–178° for B surface structures. The experimentally measured tilt angle could be an average of different surface domains present in the sample. The presence of more tilted phases during the self-assembly of alkanethiols on Ag(111) has been recently reported from time-of-flight-direct recoiling spectroscopy data [16]. This opens a more complex scenario for SAMs on Ag where different surface structures could be formed or could coexist on the sample depending on the preparation conditions such as temperature, adsorption time, or annealing procedures. Certainly, the presence of structures with different tilts can have a strong effect in applications that require a precise control of the molecule-substrate distance such as molecular electronics.

To summarize, the recently proposed [4] alternative models for the structure of the Ag(111)$(\sqrt{7}\times\sqrt{7})R19.1°$-$CH_3S$ surface phase imply a strong reconstruction of the metal topmost atomic layer which, compared to the unreconstructed commonly accepted model, would have a 3/7 density of atoms. Determining the structure and relative stability of this system is very important since it is the simplest one leading to a whole series of SAMs. From first principle atomistic thermodynamics, it is found that, in spite of the rather large difference in the atomic structure and bonding of CH_3S to the substrate, the surface free energy of the three different models involving very different reconstructions is very similar. This new and unexpected result has strong implications for the formation of SAMs, since it strongly suggests that the final SAM structure in a given experiment will strongly depend on the preparation conditions. Indeed, *in situ* STM experiments carried out for alkanethiols on Au(111) show the coexistence of different patterns [19] although without the very different reconstructions involved in the case of CH_3S on Ag(111) discussed here. More studies focusing on the dynamical aspects of SAM growth on different metallic surfaces are needed to be able to control the final structure.

Financial support has been provided by Grants No. CTQ2005-08459-CO2-01, No. UNBA05-33-001, No. CTQ2005-03222, and No. 2005SGR-00697 and *Distincio GenCat* (F. I). P. C. thanks Professor A. Muñoz for valuable support. A significant part of the computer time was provided by the Barcelona Supercomputing Center.

[1] J. C. Love *et al.*, Chem. Rev. **105**, 1103 (2005).
[2] F. Schreiber, Prog. Surf. Sci. **65**, 151 (2000).
[3] A. Ulman, Chem. Rev. **96**, 1533 (1996).
[4] M. Yu *et al.*, J. Phys. Chem. B **110**, 2164 (2006).
[5] L. H. Dubois, B. R. Zegarski, and R. G. Nuzzo, J. Chem. Phys. **98**, 678 (1993).
[6] A. L. Harris *et al.*, Phys. Rev. Lett. **64**, 2086 (1990).
[7] R. Heinz and J. P. Rabe, Langmuir **11**, 506 (1995).
[8] K. Edinger *et al.*, Langmuir **9**, 4 (1993).
[9] K. Reuter and M. Scheffler, Phys. Rev. B **65**, 035406 (2001).
[10] F. P. Cometto *et al.*, J. Phys. Chem. B **109**, 21 737 (2005).
[11] J. Perdew and Y. Wang, Phys. Rev. B **45**, 13 244 (1992).
[12] http://www.webelements.com
[13] P. Blöchl, Phys. Rev. B **50**, 17 953 (1994).
[14] H. Monkhorst and J. Pack, Phys. Rev. B **47**, 558 (1993).
[15] G. Kresse and J. Furthmuller, Phys. Rev. B **54**, 11 169 (1996).
[16] L. M. Rodriguez *et al.*, J. Phys. Chem. B **110**, 7095 (2006).
[17] J. Schnadt *et al.*, Phys. Rev. Lett. **96**, 146101 (2006).
[18] P. E. Laibinis *et al.*, J. Am. Chem. Soc. **113**, 7152 (1991).
[19] C. Vericat *et al.*, J. Chem. Phys. **115**, 6672 (2001).